

Minimum energy paths for conformational changes of viral capsids

Paolo Cermelli,^{1,*} Giuliana Indelicato,^{2,†} and Emilio Zappa^{3,‡}

¹*Dipartimento di Matematica, Università di Torino, Italy*

²*Department of Mathematics and York Centre for Complex Systems Analysis, University of York, UK and Dipartimento di Matematica, Università di Torino, Italy*

³*Courant Institute of Mathematical Sciences, New York University, USA*

Abstract

In this work we study how a viral capsid can change conformation using techniques of Large Deviations Theory for stochastic differential equations. The viral capsid is a model of a complex system in which many units - the proteins forming the capsomers - interact by weak forces to form a structure with exceptional mechanical resistance. The destabilization of such a structure is interesting both *per se*, since it is related either to infection or maturation processes, and because it yields insights into the stability of complex structures in which the constitutive elements interact by weak attractive forces. We focus here on a simplified model of a dodecahederal viral capsid, and assume that the capsomers are rigid plaquettes with one degree of freedom each. We compute the most probable transition path from the closed capsid to the final configuration using minimum energy paths, and discuss the stability of intermediate states.

* paolo.cermelli@unito.it

† giuliana.indelicato@unito.it

‡ zappa@cims.nyu.edu

I. INTRODUCTION

Viral capsids are interesting biological structures assembled from repeated copies of the same protein [1]. They are very efficient at their purpose of protecting the genetic material of the virus from the environment, since they are quite stable for a wide range of environmental conditions (cf. [2] for a review).

In order to release the genome inside the host cell, however, they must be able to change configuration and /or disassemble in response to changes in the chemical environment or the interaction with receptors of the host. Such conformational changes often involve the opening of pores in the viral shell through which the nucleic acid exits the virus and is released into the cell (see, for instance, [3–7]). More often, though, the capsid is believed to simply disassemble as a consequence of the weakening of the bonds between the capsomers [8].

Also, many viral capsids undergo changes during maturation [9]. The assembly of the capsid is often a multi-stage process that may involve various steps towards the infective, final form of the virion. Once the capsomers have assembled to form a closed shell, called procapsid, these still have to undergo conformational changes involving protein cleavage, subunit rotation and /or deformation, and substantial bond disruption and reforming, in order to reach the final, stable form of the infective virus [10].

Hence, the definition of conformational change is necessarily somewhat loose, ranging from the simple mutual detachment of the proteins leading to the complete disgregation of the capsid, to the cleavage of the capsomers triggering complex relative rigid motions of the protein subunits, to the formation of new bonds with changes in the quaternary structure of the protein.

In any event, the question arises as to which is the basic physics underlying the stability and structural plasticity of the capsid. The forces driving the conformational changes are diverse, and not always known. For instance, the RNA is highly charged and compressed within the closed capsid, and this generates an internal pressure that could destabilize the shell [10]. In other cases, there are charges on the faces of adjacent proteins that are masked by ions in the stable, closed capsid but, upon pH changes, lose the ions and trigger a Coulomb repulsion between the proteins [11]. Sometimes, instead, it is the cleavage of a particular protein that acts as switch for a conformational change of the capsomers that reach a new

stable configuration [12].

Cohesive forces that keep the capsid together are also diverse: there are no covalent bonds between the capsomers, but binding can involve strong hydrophobic bonds between chains 'knotted' around or inside beta barrels of adjacent proteins, hydrogen bonds, Coulomb attraction, and so on [13].

What is clear, though, is the cooperative nature of the stability of the capsid. The bonds keeping the capsomer together must be comparatively weak in order to allow for easy and fast configurational changes, and the secret of the capsid stability must lie in the joint stabilizing action of adjacent capsomers upon each other [4, 9, 12, 14].

In this work we continue the investigation started in [15, 16] (cf. also ([17])), to study under which conditions configurational changes in viral capsids involve either simultaneous collective movements, or completely disordered unrelated events, or a cascade of local destabilization events leading to a wavefront propagating along the shell.

We use here the formalism of Large Deviations Theory [18] to explore the energy landscape and the minimum energy paths between metastable states. The formalism provides both a solid theoretical framework to study transitions, and a numerical procedure to characterize the most probable paths [19–22].

We prove that, under quite general hypotheses on the energy function, the conformational change occurs by a domino effect in which local destabilization events trigger their neighbors, and this propagates along the capsid until completion. This is confirmed by linearizing the model and computing the stationary distribution of fluctuations around metastable states: the concentration matrix shows that only adjacent pentamers are correlated. Explicit results for a special form of the capsid energy are presented and discussed.

We use here a simplified model of viral capsid, and make strong simplifying assumptions on the form of the interaction energy between the capsomers, because what we are really interested in is the basic principle leading to destabilization in structures in which stability is a cooperative affair.

Clearly, our results rely on, in addition to the form of the interaction energies, the topology of the network of interactions between the capsomers, and can be easily generalized to other, more general, networks.

II. THE DODECAHEDRAL MODEL

In the simplified model studied in this paper the capsid is described as a dodecahedron \mathcal{C} (see Figure 1). We assume that every configuration of the capsid is described by an order parameter $\mathbf{x} = (x_1, \dots, x_{12})$, with indexing corresponding to a labeling of the faces as in Figure 1, where $x_i \in \mathbb{R}$ is a variable describing the state of each pentagonal unit. For instance, in destabilization problems leading to the opening of the capsid during the infection process, we can assume that each pentagonal face of the dodecahedron \mathcal{C} is a rigid plaquette that can only translate along an axis orthogonal to its plane, and choose x_i as its radial displacement.

In order to account for interactions between adjacent pentagons, it is convenient to work on the dual graph G of \mathcal{C} , which has the property that the vertices of G correspond to the faces of \mathcal{C} , the edges of G to the edges of \mathcal{C} and the faces of G to the vertices of \mathcal{C} . G is the graph of the icosahedron, and $\delta = 5$ is the common degree of all vertices of the graph. From now on we view \mathbf{x} as a field on the vertices of the icosahedral graph G .

Denoting by $V = \{1, \dots, 12\}$ and E the sets of vertices and edges of G , respectively, the adjacency matrix is the square symmetric 12×12 matrix defined by

$$A_{ij} = \begin{cases} 1 & \text{if } ij \in E \\ 0 & \text{otherwise,} \end{cases} \quad i, j \in \{1, \dots, 12\}.$$

Notice that the ij -entry of the adjacency matrix A of G is not vanishing if and only if the i and j faces of the dodecahedron \mathcal{C} meet at a common edge.

We say that a map $V \rightarrow V$ is an automorphism of G if it is one-to-one and if it and its inverse maps adjacent vertices into adjacent vertices. The group of automorphisms of the icosahedral graph G is the Coxeter group $\mathcal{H}_3 = \mathcal{I} \times \mathbb{Z}_2$ of order 120, where \mathcal{I} denotes the rotational group of the icosahedron, with order 60 [23]. The group \mathcal{I} acts on the vertices of G , which are the faces of \mathcal{C} , inducing a permutation representation (perm rep) $\sigma : \mathcal{I} \rightarrow S_{12}$, where S_{12} is the symmetric group over 12 elements. The perm rep σ induces a representation $\rho : \mathcal{I} \rightarrow GL(12, \mathbb{R})$, given by

$$\rho(g)\mathbf{e}_j := \mathbf{e}_{\sigma(g)(j)}, \quad g \in \mathcal{I},$$

where $\mathbf{e}_j, j = 1, \dots, 12$ denotes the standard basis of \mathbb{R}^{12} .

The direct product decomposition of \mathcal{H}_3 implies that the representation

$$\tilde{\rho} = \rho \otimes \Gamma, \quad (1)$$

is a representation of \mathcal{H}_3 . Here $\Gamma = \{\pm 1\}$ is a representation of \mathbb{Z}_2 and \otimes denotes the tensor product of representations (in this case, since the groups are finite, this is the Kronecker product of matrices) [24]. Since \mathcal{H}_3 is the automorphism group of G , we have

$$[A, \tilde{\rho}(g)] = 0, \quad \forall g \in \mathcal{H}_3,$$

where $[,]$ denotes the commutator in $GL(12, \mathbb{R})$. In other words, A commutes with all the matrices of $\tilde{\rho}(\mathcal{H}_3)$.

There is a connection between the eigenspaces of A and the decomposition into irreducible representations (irreps) of $\tilde{\rho}$ [26]. The character table of \mathcal{I} is given by

Irrep	$C(e)$	$C(g_5)$	$C(g_5^2)$	$C(g_2)$	$C(g_2g_5)$
ρ_1	1	1	1	1	1
ρ_2	3	τ	$1-\tau$	-1	0
ρ_3	3	$1-\tau$	τ	-1	0
ρ_4	4	-1	-1	0	1
ρ_5	5	0	0	1	-1

where $\tau = \frac{1+\sqrt{5}}{2}$ is the golden ratio, g_2 and g_5 a two- and five-fold rotation of the icosahedron, respectively, and C denotes the conjugacy class of an element of the group. The decomposition of $\tilde{\rho}$ into irreps is given by [25]

$$\hat{\rho} = \bigoplus_{i=1,2,3,5} \rho_i \otimes \Gamma,$$

and there exists a matrix $R \in GL(12, \mathbb{R})$ such that $R^{-1}\tilde{\rho}R = \hat{\rho}$. The explicit form of R is given in [25]. It is shown in [26] that the matrix R diagonalises the adjacency matrix A of the graph G ; in particular, the spectrum of A is given by

Eigenvalue	Dimension	Irrep
5	1	ρ_1
$\sqrt{5}$	3	ρ_2
$-\sqrt{5}$	3	ρ_3
-1	5	ρ_5

III. ENERGY

We associate with the capsid an energy function $E : \mathbb{R}^{12} \rightarrow \mathbb{R}$ that we require to be invariant under the action $\tilde{\rho}(\mathcal{H}_3)$ of the symmetry group of the capsid [25]. Writing, with a slight abuse of notation, $\tilde{\rho}(\mathcal{H}_3) \subset GL(12, \mathbb{R})$ simply as \mathcal{H}_3 , this means that

$$E(H\mathbf{x}) = E(\mathbf{x}), \quad \forall H \in \mathcal{H}_3, \forall \mathbf{x} \in \mathbb{R}^{12}, \quad (2)$$

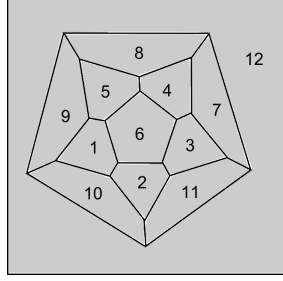


FIG. 1. Schlegel diagram of the dodecahedron with the indexing convention used here.

which implies that the gradient $\nabla E(\mathbf{x})$ is equivariant with respect to \mathcal{H}_3 , i.e.

$$\nabla(E(H\mathbf{x})) = H\nabla E(\mathbf{x}), \quad \forall H \in \mathcal{H}_3. \quad (3)$$

We assume that conformational changes of the capsid result from the competition between a driving force on each pentamer and a counteracting interaction force between adjacent pentamers, and write the total energy of the capsid as

$$E(\mathbf{x}) = \sum_{i=1}^{12} f(x_i) + \gamma \sum_{i,j=1}^{12} A_{ij} g(x_i, x_j), \quad \gamma \in \mathbb{R}, \quad (4)$$

with $f : \mathbb{R} \rightarrow \mathbb{R}$ and $g : \mathbb{R}^2 \rightarrow \mathbb{R}$ to be specified below. For problems involving the opening of the capsid, f is the expansion energy and g is the attractive energy acting at pentamer interfaces. The constant γ is a real parameter controlling the stability of the capsid. Notice that $E(\mathbf{x})$ is invariant under \mathcal{H}_3 , so that (2) and (3) hold.

We require that $f : \mathbb{R} \rightarrow \mathbb{R}$ and $g : \mathbb{R}^2 \rightarrow \mathbb{R}$ be smooth and

A_1 the expansion energy is convex, has an absolute minimum at state $\bar{x} = 1$, and $f(1) = f'(1) = 0$, $f''(1) > 0$. When $x_i = 1$, we say that pentamer i has switched to the final conformation and is in state 1. In detachment problems where x_i is the displacement along the capsomer axis, it would be more appropriate to assume that the expansion energy f is monotone decreasing, and there is a cutoff value \bar{x} such that f vanishes identically for $x \geq \bar{x}$. However, the analysis does not change if we assume that each pentamer cannot detach further than \bar{x} , and assume that this corresponds to an isolated minimum of f .

A_2 the interaction energy $g = g(x, y)$ has a unique strict global minimum at $x = y = 0$ and is symmetric, i.e., $g(x, y) = g(y, x)$. Further, writing $g_1 = \frac{\partial g}{\partial x}$, $g_2 = \frac{\partial g}{\partial y}$, $g_{11} = \frac{\partial^2 g}{\partial x^2}$,

and $g_{12} = \frac{\partial^2 g}{\partial x \partial y}$, we require that $g_1(x, x) \geq 0$ and $g_{12}(x, x) < 0$ for every $x > 0$, and there is a cutoff value $\bar{d} \ll 1$ such that g vanishes identically for $x^2 + y^2 \geq \bar{d}^2$. Hence, the interaction energy has much shorter radius than the expansive energy. In particular, $g(x, y)$ and all its derivatives vanish identically when one of the arguments equals 1.

We remark that both energies vanish identically when a component x_i is equal to 1. As mentioned above, we identify states such that $x_i = 1$ as states where the corresponding pentamer has switched to its final state, either by changing its conformation, or by detaching from the capsid, depending on the problem at hand. On the other hand, pentamers such that $x_i \sim 0$ will be viewed as being in the initial, or attached state, and will be said to be in state 0.

We assume that every minimum of the energy is uniquely characterized by the corresponding combination of pentamers that are in state 1, i.e., by its combination of components that equal 1. Formally,

A_3 if two minima of the energy $\hat{\mathbf{x}}$ and $\tilde{\mathbf{x}}$ are such that, for each i , either $\hat{x}_i = \tilde{x}_i = 1$ or $\hat{x}_i, \tilde{x}_i < 1$, then $\hat{\mathbf{x}} = \tilde{\mathbf{x}}$.

A_4 if two minima of the energy $\hat{\mathbf{x}}$ and $\tilde{\mathbf{x}}$ do not belong to the same icosahedral orbit, then $E(\hat{\mathbf{x}}) \neq E(\tilde{\mathbf{x}})$: in other words, each minimum (modulo symmetry) is characterized by a unique energy level.

A. Icosahedral minima

In this section we partially characterize the changes of the energy landscape resulting from variations of the bond strength γ . First notice that assumption A_3 implies that there is at most equilibrium in which all pentamers are in the initial state, such that $x_i \neq 1$ for all i . Using the result (28) it follows that this equilibrium has full icosahedral symmetry, i.e., $x_i = x_0$, for all $i = 1, \dots, 12$.

The gradient and the Hessian of the energy are

$$\frac{\partial E}{\partial x_i}(\mathbf{x}) = f'(x_i) + 2\gamma \sum_{j=1}^{12} A_{ij} g_1(x_i, x_j), \quad i = 1, \dots, 12. \quad (5)$$

and

$$\begin{aligned}\frac{\partial^2 E}{\partial x_i^2}(\mathbf{x}) &= f''(x_i) + 2\gamma \sum_{j=1}^{12} A_{ij} g_{11}(x_i, x_j), \\ \frac{\partial^2 E}{\partial x_i \partial x_j}(\mathbf{x}) &= 2\gamma A_{ij} g_{12}(x_i, x_j).\end{aligned}\tag{6}$$

Then x_0 must be a solution of the equation

$$h(x) = f'(x) + 10\gamma g_1(x, x) = 0.\tag{7}$$

The above equation has always the solution $x = 1$, i.e., the configuration in which all pentamers have switched to state 1. Further, by A_2 , the function $g_1(x, x)$ is nonnegative and $g_1(0, 0) = g_1(1, 1) = 0$. Since $f'(x) < 0$ for $x < 1$, then there exists a critical value γ_c such that for $\gamma > \gamma_c$ there are two solutions $x_s = x_s(\gamma) < 1$ and $x_u = x_u(\gamma) < 1$ of (7), with the property that $h'(x_s) > 0$ and $h'(x_u) < 0$, while for $\gamma < \gamma_c$ there are no solutions. Hence, the system undergoes a saddle-node bifurcation at γ_c .

The Hessian of the energy computed at an isotropic state $x_i = x$ for all i is

$$aI + bA,$$

with $a = a(x) = f''(x) + 10\gamma g_{11}(x, x)$ and $b = b(x) = 2\gamma g_{12}(x, x)$. Notice that, by our hypotheses on g, f , we have that $b(x) < 0$, and the Hessian is proportional to the adjacency matrix A of the graph (modulo the addition of a multiple of the identity). Therefore, its eigenspaces are also associated with the irreps of the representation $\tilde{\rho}$ of \mathcal{H}_3 as in (1). The eigenvalues of the Hessian listed in increasing order are

Eigenvalue	Dimension	Irrep
$\mu_1 = a + 5b$	1	ρ_1
$\mu_2 = a + b\sqrt{5}$	3	ρ_2
$\mu_3 = a - b$	5	ρ_5
$\mu_4 = a - b\sqrt{5}$	3	ρ_3

Hence,

$$h'(x) = a(x) + 5b(x) = \mu_1,$$

is the minimum eigenvalue of the Hessian, so that for $\gamma > \gamma_c$ the first critical point x_s is a relative minimum of the energy, since the minimum eigenvalue $\mu_1(x_s)$ of the Hessian is positive. A similar argument shows that x_u is a saddle point. Notice also that, at the bifurcation point, the smallest eigenvalue of the Hessian changes sign, and the associated eigenspace is the isotropic line: hence, destabilization at the critical value γ_c occurs by a breathing expansive mode.

IV. CONFORMATIONAL CHANGES

In many cases, the changes of conformation of the capsid are triggered by variations of the chemical environment of the virion, which modifies the interactions between the proteins and, by consequence, the energy function. In our simplified model, such changes are reckoned by variations of the parameter γ .

However, the simple saddle-node bifurcation occurring at γ_c , in which the destabilization occurs via an icosahedrally symmetric expansion, does not account for the complexity of the interactions between the capsomers. In fact, the cooperative nature of the stability of the capsid suggests that the destabilization occurs as a cascade of elementary events: the switching of single capsomers requires less energy than the simultaneous change of state of all of them, and once one of them has switched, its neighbors are destabilized and a cascade of destabilization event is triggered, with decreasing energy barriers as the number of unswitched pentamers decreases.

A possible way to study the destabilization cascade is to work in the stable regime, and to treat the process in terms of a path visiting the metastable states of the energy according to the law of rare events, using Large Deviations Theory (LDT) for stochastic dynamical systems. In other terms, we assume that, near the initial-state equilibrium, additive fluctuations of the system due to changes of the environment are able to drive it out of equilibrium, with increasing probability as $\gamma \rightarrow \gamma_c$, and the actual conformational change can be described by this stochastic process.

Hence, we assume from now on that $\gamma > \gamma_c$, and denote by $\mathbf{x}_0 = (x_s, \dots, x_s)$ the icosahedral minimum of the energy E for which $x_s < 1$, and by $\mathbf{x}_1 = (1, \dots, 1)$ the final-state icosahedral minimum. In problems involving the opening of the capsid, \mathbf{x}_0 and \mathbf{x}_1 correspond to the closed and open capsid, respectively.

Consider first the deterministic dissipative gradient-flow dynamics

$$\dot{\mathbf{x}} = -\nabla E(\mathbf{x}), \quad (8)$$

where the superposed dot denotes differentiation with respect to time $t \in \mathbb{R}^+$, and $\mathbf{x} = \mathbf{x}(t)$ is the motion in the configuration space \mathbb{R}^{12} . Since $\gamma > \gamma_c$, the system (8) has an attractor at $\mathbf{x} = \mathbf{x}_0$ (i.e., $x_i = x_0 = x_s \ \forall i$): the initial state is stable for the dynamics (8), and every small perturbation of this state tends to vanish over finite time intervals.

Now, let $\mathbf{W} = (W^{(1)}(t), \dots, W^{(12)}(t))$ be a 12-dimensional Brownian motion defined on a probability space $(\Omega, \mathcal{A}, \mathbb{P})$. We consider random perturbations of the dynamical system (8), by superimposing an additive noise $dW^{(i)}$ to each face i of the polyhedron \mathcal{C} . This results in the stochastic differential equation

$$d\mathbf{x} = -\nabla E(\mathbf{x})dt + \epsilon d\mathbf{W}, \quad (9)$$

with $\epsilon > 0$ a small parameter.

A. Results from large deviations theory

In this section we briefly review some key concepts from LDT that we are going to use throughout the paper. We refer to [18] for more information.

The main object of LDT is the action functional $S_T(\varphi)$ which, for the equation (9), is given by

$$S_T(\varphi) = \int_0^T |\dot{\varphi} + \nabla E(\varphi)|^2 dt, \quad (10)$$

where $T > 0$ and $\varphi : [0, T] \rightarrow \mathbb{R}^{12}$ is an absolutely continuous path (actually, the functional is defined on continuous paths, but its value is $+\infty$ if φ is not absolutely continuous). The LDT states that, given a bounded set $D \subseteq \mathbb{R}^{12}$, then the probability $\mathbb{P}^{\mathbf{x}}(\mathbf{x}(T) \in D)$ that the solution $\mathbf{x}(T)$ of (9) belongs to D given that $\mathbf{x}(0) = \mathbf{x}$ satisfies

$$\lim_{\epsilon \rightarrow 0} \epsilon^2 \ln \mathbb{P}^{\mathbf{x}}(\mathbf{x}(T) \in D) = - \min_{\varphi \in \mathcal{C}_{\mathbf{x}, D}} S_T(\varphi),$$

where $\mathcal{C}_{\mathbf{x}, D} = \{\varphi \in \mathcal{C}([0, T], \mathbb{R}^{12}) : \varphi(0) = \mathbf{x}, \varphi(T) \in D\}$. If the event occurs, then $\mathbf{x}(t)$ is arbitrarily close to the minimizer

$$\varphi^* = \arg \min_{\varphi \in \mathcal{C}_{\mathbf{x}, D}} S_T(\varphi), \quad (11)$$

in the sense that, for every $\delta > 0$,

$$\lim_{\epsilon \rightarrow 0} \mathbb{P}^{\mathbf{x}} \left(\sup_{0 \leq t \leq T} |\varphi^*(t) - \mathbf{x}(t)| < \delta \middle| \mathbf{x}(T) \in D \right) = 1.$$

Another central object in LDT is the quasipotential

$$V(\mathbf{x}, \mathbf{y}) = \inf_{T > 0} \min_{\varphi \in \mathcal{C}_{\mathbf{x}, \mathbf{y}}} S_T(\varphi), \quad (12)$$

where $\mathcal{C}_{\mathbf{x}, \mathbf{y}} = \{\boldsymbol{\varphi} \in \mathcal{C}([0, T], \mathbb{R}^{12}) : \boldsymbol{\varphi}(0) = \mathbf{x}, \boldsymbol{\varphi}(T) = \mathbf{y}\}$. For large time intervals, if \mathbf{x}_0 is the unique stable point of (8), the density $p(\mathbf{x})$ associated with the stationary distribution of (9), provided it exists, is such that

$$p(\mathbf{x}) \asymp \frac{1}{Z} \exp \left(-\frac{V(\mathbf{x}_0, \mathbf{x})}{\epsilon^2} \right), \quad (13)$$

where Z is a normalization constant. Here \asymp denotes the log-asymptotic equivalence for $\epsilon \rightarrow 0$, i.e. $\lim_{\epsilon \rightarrow 0} \epsilon^2 \ln(p(\mathbf{x})) = -V(\mathbf{x}_0, \mathbf{x})$. For a gradient system like (9), the quasipotential at a point \mathbf{x} lying in the basin of attraction of a minimum \mathbf{x}_0 of E is given by

$$V(\mathbf{x}_0, \mathbf{x}) = 2(E(\mathbf{x}) - E(\mathbf{x}_0)). \quad (14)$$

Suppose \mathbf{x}_A and \mathbf{x}_B are two (local) minima of E separated by a single saddle point \mathbf{x}_S . Then the minimizer $\boldsymbol{\varphi}^*$ of the action functional $S_T(\boldsymbol{\varphi})$ with $\boldsymbol{\varphi}(0) = \mathbf{x}_A$ and $\boldsymbol{\varphi}(T) = \mathbf{x}_B$ is the path such that, up to a normalization constant,

$$(\nabla E)^\perp(\boldsymbol{\varphi}^*) = \mathbf{0}, \quad (15)$$

where $(\nabla E)^\perp$ is the component of ∇E normal to $\boldsymbol{\varphi}^*$:

$$(\nabla E)^\perp(\boldsymbol{\varphi}^*) = \nabla E(\boldsymbol{\varphi}^*) - \langle \nabla E(\boldsymbol{\varphi}^*), \hat{\boldsymbol{\tau}} \rangle \hat{\boldsymbol{\tau}}, \quad (16)$$

where $\hat{\boldsymbol{\tau}}$ is the unit tangent of $\boldsymbol{\varphi}^*$ and $\langle \cdot, \cdot \rangle$ denotes the standard Euclidean product. The path $\boldsymbol{\varphi}^*$ is referred to as the Minimum Energy Path (MEP) connecting \mathbf{x}_A and \mathbf{x}_B [19].

The dynamics of (9) on the energy landscape can be modeled as a continuous time Markov chain with states the minima of $E(\mathbf{x})$ [18, 27]. In this framework, two minima \mathbf{x}_α and \mathbf{x}_β are connected if the minimizer of $S_T(\boldsymbol{\varphi})$ corresponds to the MEP $\boldsymbol{\varphi}^*$ with a single maximal value of the energy along it. The off-diagonal entries of the generator matrix Q of the chain are given by

$$Q_{\alpha\beta} = \begin{cases} \exp \left(-\frac{2}{\epsilon^2} (E(\mathbf{x}_{\alpha\beta}) - E(\mathbf{x}_\alpha)) \right) & \text{if } \mathbf{x}_\alpha \text{ and } \mathbf{x}_\beta \text{ are connected} \\ 0 & \text{otherwise} \end{cases} \quad (17)$$

where $\mathbf{x}_{\alpha\beta}$ is the unique saddle point between \mathbf{x}_α and \mathbf{x}_β . The diagonal entries are chosen such that the sum of each row is zero:

$$Q_{\alpha\alpha} = - \sum_{\beta \neq \alpha} Q_{\alpha\beta}.$$

The jump matrix Π is obtained from Q by setting

$$\Pi_{\alpha\alpha} = 0, \quad \Pi_{\alpha\beta} = -\frac{Q_{\alpha\beta}}{Q_{\alpha\alpha}}, \quad \alpha \neq \beta. \quad (18)$$

The jump matrix Π is the generator matrix of a discrete Markov chain [28]. Following [27], we introduce the limiting jump matrix (or zero-temperature jump matrix)

$$\Pi_0 = \lim_{\epsilon \rightarrow 0} \Pi. \quad (19)$$

The limiting jump matrix depends only on the values of the potential at the saddles [27].

B. Admissible states

The energy landscape is complex and there are many local minima, among which the icosahedral minimum. By assumption A_3 , local minima are completely characterized by the combination of pentamers i such that $x_i = 1$, and $0 < x_j \ll 1$ for the remaining indices.

We parametrize the minima by strings $\mathbf{s} \in \{0, 1\}^{12}$, where $s_i = 1$ means that the pentagon i is in state 1, for instance detached from the capsid, while $s_i = 0$ means that the pentagon is still in its initial state, for instance attached to its neighbors. Precisely, we say that a state \mathbf{s} is *admissible* if it belongs to the basin of attraction of a critical point $\hat{\mathbf{x}}(\mathbf{s})$ of the dynamical system (8) that corresponds to the same combination of pentamers in state 1 as \mathbf{s} , i.e., if

$$\mathbf{s} \in S \Leftrightarrow \begin{cases} \lim_{t \rightarrow +\infty} \mathbf{x}(t, \mathbf{s}) = \hat{\mathbf{x}}(\mathbf{s}), \\ s_i = 1 \Leftrightarrow \hat{x}_i(\mathbf{s}) = 1, \\ s_i = 0 \Leftrightarrow \hat{x}_i(\mathbf{s}) < 1, \end{cases} \quad (20)$$

where $\mathbf{x}(t, \mathbf{s})$ is the solution of (8) with initial conditions $\mathbf{x}(0) = \mathbf{s}$.

We denote by S the set of admissible states, and write $\sum_i s_i$ for the number of pentamers in state 1. Special admissible states are the initial configuration $\mathbf{s}_0 = (0, 0, \dots, 0)$ and the final configuration $\mathbf{s}_1 = (1, 1, \dots, 1)$.

As an example, a set of admissible states for the energy (39) is shown in Figure 4. These are obtained by solving numerically the dynamical system (8) with initial conditions $\mathbf{x}(0) = \mathbf{s}$, to determine the attractor $\hat{\mathbf{x}}(\mathbf{s})$ whose basin $\mathbf{x}(0)$ belongs to.

As seen in Section IV A, the dynamics on the energy landscape can be analyzed by defining a Markov chain on the S of admissible states. This analysis is carried out in the next section.

C. Transitions

Given two admissible states $\mathbf{s}, \mathbf{s}' \in S$, we say that $\mathbf{s} < \mathbf{s}'$ if $s'_i = 1$ when $s_i = 1$ and $\sum_i s_i < \sum_i s'_i$: in this case, since pentamers that are in state 1 in \mathbf{s} are also in state 1 in \mathbf{s}' , the state \mathbf{s}' is obtained by switching to 1 some of the pentamers that are in state 0 in \mathbf{s} . The relation $<$ induces a strict partial order on the set S consistent with the structure of directed graph below.

We say that there is a directed edge between two admissible states \mathbf{s} , and \mathbf{s}' , and write $\mathbf{s} \rightarrow \mathbf{s}'$, if

- i) $\mathbf{s}' > \mathbf{s}$, so that no reverse transition or reattachment of pentamers is allowed; and
- ii) there is a MEP connecting the corresponding minima $\hat{\mathbf{x}}(\mathbf{s}), \hat{\mathbf{x}}(\mathbf{s}')$, along which the energy has a single maximum, as described in Section IV A.

Requirement (i) is strongly restrictive, in that it excludes conformational changes involving pentamers going back to their initial configuration, or reattaching to the capsid. According to LDT, such transitions are indeed possible in the stochastic dynamics (9) and this may give rise to cycles. The Markov chain that we construct below, however, is meant to describe a restricted situation in which configurational changes are irreversible, as is the case for most configurational changes in capsids, first of all the disaggregation. In other terms, the values $x_i = 1$ act as absorbing states for the i -th component of SDE (9).

If \mathbf{x}_m is the point of the MEP between $\hat{\mathbf{x}}(\mathbf{s})$ and $\hat{\mathbf{x}}(\mathbf{s}')$ where the maximum is attained, we define the barrier between \mathbf{s} and \mathbf{s}' by

$$\beta(\mathbf{s}, \mathbf{s}') = V(\hat{\mathbf{x}}(\mathbf{s}), \mathbf{x}_m) = 2(E(\mathbf{x}_m) - E(\hat{\mathbf{x}}(\mathbf{s}))), \quad \text{if } \mathbf{s} \rightarrow \mathbf{s}', \quad (21)$$

which is positive by construction. We set $\beta(\mathbf{s}, \mathbf{s}') = +\infty$ if \mathbf{s} is not connected to \mathbf{s}' .

The above procedure endows the set S with a structure of directed acyclic graph with positive weights. To construct explicitly the weights β , the MEP between any pair of states can be determined using the numerical procedure introduced in [19–21], taking for instance as initial path the straight line joining $\hat{\mathbf{x}}(\mathbf{s})$ to $\hat{\mathbf{x}}(\mathbf{s}')$.

D. The Markov chain

In order to describe the dynamics on the energy landscape and determine the most probable transitions paths, as discussed in Section IV A we construct a Markov chain on the state space S . The generator matrix Q of this chain is given by (compare with (17))

$$Q(\mathbf{s}, \mathbf{s}') = \begin{cases} \exp\left(-\frac{1}{\epsilon^2}\beta(\mathbf{s}, \mathbf{s}')\right) & \text{if } \mathbf{s} \rightarrow \mathbf{s}', \\ 0 & \text{otherwise,} \end{cases}$$

and

$$Q(\mathbf{s}, \mathbf{s}) = - \sum_{\mathbf{s}' : \mathbf{s} \rightarrow \mathbf{s}'} Q(\mathbf{s}, \mathbf{s}').$$

The jump matrix Π as in (18) is then given by

$$\Pi(\mathbf{s}, \mathbf{s}') = -\frac{Q(\mathbf{s}, \mathbf{s}')}{Q(\mathbf{s}, \mathbf{s})} = \frac{\exp\left(-\frac{\beta(\mathbf{s}, \mathbf{s}')}{\epsilon^2}\right)}{\sum_{\mathbf{s} \rightarrow \mathbf{s}''} \exp\left(-\frac{\beta(\mathbf{s}, \mathbf{s}'')}{\epsilon^2}\right)}, \quad \Pi(\mathbf{s}, \mathbf{s}) = 0. \quad (22)$$

Letting $\epsilon \rightarrow 0$ we obtain the zero-temperature jump matrix (cf. (19))

$$\Pi_0(\mathbf{s}, \mathbf{s}') = \lim_{\epsilon \rightarrow 0} \Pi(\mathbf{s}, \mathbf{s}'). \quad (23)$$

The matrix Π_0 defines a Markov chain on the set of admissible states S by assuming that the transition probability between the states \mathbf{s}, \mathbf{s}' is

$$\pi(\mathbf{s}' | \mathbf{s}) = \Pi_0(\mathbf{s}, \mathbf{s}'). \quad (24)$$

The explicit form of the matrix Π_0 is the following:

$$\begin{aligned} \Pi_0(\mathbf{s}, \mathbf{s}') &= \lim_{\epsilon \rightarrow 0} \frac{1}{\sum_{\mathbf{s} \rightarrow \mathbf{s}''} \exp\left(-\frac{(\beta(\mathbf{s}, \mathbf{s}'') - \beta(\mathbf{s}, \mathbf{s}'))}{\epsilon^2}\right)} \\ &= \begin{cases} \frac{1}{N(\mathbf{s})} & \text{if } \mathbf{s} \rightarrow \mathbf{s}' \text{ and } \beta(\mathbf{s}, \mathbf{s}') = \min_{\mathbf{s} \rightarrow \mathbf{s}''} \beta(\mathbf{s}, \mathbf{s}'') \\ 0 & \text{otherwise} \end{cases} \end{aligned} \quad (25)$$

where $N(\mathbf{s}) = |\{\mathbf{s}' : \beta(\mathbf{s}, \mathbf{s}') = \min_{\mathbf{s} \rightarrow \mathbf{s}''} \beta(\mathbf{s}, \mathbf{s}'')\}|$ is the number of states that can be reached from \mathbf{s} along a path with minimum barrier.

The most probable transition path between the closed state \mathbf{s}_0 to the open state \mathbf{s}_1 is the realization of the chain that maximizes the transition probability at each step, i.e., the path along which the barriers are minimal among all the admissible transitions outgoing from each vertex (cf. Theorem 6.6.1 in [18]).

V. REDUCTION BY SYMMETRY

Since the energy E is invariant under the action of the symmetry group \mathcal{H}_3 , minima are mapped into minima by \mathcal{H}_3 , and this induces a permutation action on the set of minima of E . By (3) and uniqueness of the solution of (8), if $\mathbf{x}(t)$ is the solution of (8) with initial condition \mathbf{s} , then $H\mathbf{x}(t)$ is the solution of (8) with initial condition $H\mathbf{s}$, for every $H \in \mathcal{H}_3$, and hence, by (20), it follows that

$$\mathbf{s}' = H\mathbf{s} \Leftrightarrow \hat{\mathbf{x}}(\mathbf{s}') = H\hat{\mathbf{x}}(\mathbf{s}), \quad H \in \mathcal{H}_3, \quad (26)$$

so that, in turn, \mathcal{H}_3 acts on S . Denoting by

$$\text{Fix}(\mathbf{s}) = \{H \in \mathcal{H}_3 : H\mathbf{s} = \mathbf{s}\}$$

the isotropy group of \mathbf{s} , (26) implies that $\hat{\mathbf{x}}(\mathbf{s})$ is invariant under $\text{Fix}(\mathbf{s})$, i.e.,

$$\hat{\mathbf{x}}(\mathbf{s}) = H\hat{\mathbf{x}}(\mathbf{s}), \quad H \in \text{Fix}(\mathbf{s}), \quad (27)$$

which in turn implies that $\hat{\mathbf{x}}(\mathbf{s}_0)$ and $\hat{\mathbf{x}}(\mathbf{s}_1)$ have all components equal, since $\text{Fix}(\mathbf{s}_0) = \text{Fix}(\mathbf{s}_1) = \mathcal{H}_3$ and therefore

$$\hat{\mathbf{x}}(\mathbf{s}_0) = H\hat{\mathbf{x}}(\mathbf{s}_0), \quad \hat{\mathbf{x}}(\mathbf{s}_1) = H\hat{\mathbf{x}}(\mathbf{s}_1), \quad H \in \mathcal{H}_3, \quad (28)$$

The set S therefore can be decomposed into orbits of \mathcal{H}_3 . We denote by Σ the set S/\mathcal{H}_3 . Figure 4 shows the reduced state space Σ for the energy (39). We now show that the Markov chain Π on S induces a Markov chain $\tilde{\Pi}$ on Σ .

Consider first a MEP φ^* connecting two minima \mathbf{x}_0 and \mathbf{x}_1 : by construction, φ^* is a minimizer of the action function $S_T(\varphi)$ as in (10). Since E is invariant under \mathcal{H}_3 , by (3) $\nabla E(H\mathbf{x}) = H\nabla E(\mathbf{x})$ for $H \in \mathcal{H}_3$, and therefore, since H is orthogonal, $S_T(\varphi) = S_T(H\varphi)$. This means that if φ^* is a MEP from \mathbf{x}_0 to \mathbf{x}_1 , then $H\varphi^*$ is a MEP from $H\mathbf{x}_0$ to $H\mathbf{x}_1$. Hence, noting that $\mathbf{s} < \mathbf{s}'$ implies $H\mathbf{s} < H\mathbf{s}'$,

$$\mathbf{s} \rightarrow \mathbf{s}' \Rightarrow H\mathbf{s} \rightarrow H\mathbf{s}' \quad H \in \mathcal{H}_3. \quad (29)$$

We now prove a basic property of barriers. From the invariance of E and the above discussion, it follows that $E(\varphi(s)) = E(H\varphi(s))$ for every $s \in [0, T]$, and using (26) and (21) this shows that

$$\beta(H\mathbf{s}, H\mathbf{s}') = \beta(\mathbf{s}, \mathbf{s}'), \quad H \in \mathcal{H}_3. \quad (30)$$

Notice in particular that, denoting by $\text{Fix}(\mathbf{s}) = \{H \in \mathcal{H}_3 : H\mathbf{s} = \mathbf{s}\}$ the isotropy group of \mathbf{s} ,

$$\mathbf{s} \rightarrow \mathbf{s}' \Rightarrow \mathbf{s} \rightarrow H\mathbf{s}' \quad \text{and} \quad \beta(\mathbf{s}, H\mathbf{s}') = \beta(\mathbf{s}, \mathbf{s}'), \quad H \in \text{Fix}(\mathbf{s}). \quad (31)$$

Hence, the value of the barrier between the state \mathbf{s} and all states in $\text{Fix}(\mathbf{s})\mathbf{s}'$ is the same.

We define a weighted graph with vertex set Σ as follows: for $\sigma, \sigma' \in \Sigma$, we write

$$\sigma \rightarrow \sigma' \quad \text{with weight} \quad \tilde{\beta}(\sigma, \sigma') \quad (32)$$

if there exist $\mathbf{s} \in \sigma, \mathbf{s}' \in \sigma'$ such that

$$\mathbf{s} \rightarrow \mathbf{s}' \quad (33)$$

in which case we write

$$\tilde{\beta}(\sigma, \sigma') = \min_{\mathbf{s}' \in \sigma'} \beta(\mathbf{s}, \mathbf{s}'). \quad (34)$$

The above definition is well given. In fact, let $\mathbf{s}' \in \sigma'$ such that $\beta(\mathbf{s}, \mathbf{s}') = \min_{\mathbf{s}'' \in \sigma'} \beta(\mathbf{s}, \mathbf{s}'')$, and assume that there exist $\mathbf{t} \in \sigma, \mathbf{t}' \in \sigma'$ such that $\beta(\mathbf{t}, \mathbf{t}') = \min_{\mathbf{t}'' \in \sigma'} \beta(\mathbf{t}, \mathbf{t}'') \neq \beta(\mathbf{s}, \mathbf{s}')$. Then by transitivity on the orbits there exists $H \in \mathcal{H}_3$ such that $\mathbf{t} = H\mathbf{s}$, so that by (30) $\beta(\mathbf{t}, \mathbf{t}'') = \beta(\mathbf{s}, H^\top \mathbf{t}')$. Clearly, $H^\top \mathbf{t}' \in \sigma'$ and this implies that $\beta(\mathbf{s}, \mathbf{s}') \leq \beta(\mathbf{t}, \mathbf{t}'')$. Since the converse also holds, we arrive at a contradiction and $\beta(\mathbf{s}, \mathbf{s}') = \beta(\mathbf{t}, \mathbf{t}')$.

The above construction defines a Markov chain $\tilde{\Pi}$ on Σ :

$$\tilde{\Pi}(\sigma, \sigma') = \frac{\exp\left(-\frac{\tilde{\beta}(\sigma, \sigma')}{\epsilon^2}\right)}{\sum_{\sigma \rightarrow \sigma''} \exp\left(-\frac{\tilde{\beta}(\sigma, \sigma'')}{\epsilon^2}\right)}, \quad \tilde{\Pi}(\sigma, \sigma) = 0. \quad (35)$$

To compute the low-temperature limit of (35), we make a further assumption on the system:

A₅ For every admissible state \mathbf{s} , if $\beta(\mathbf{s}, \mathbf{s}') = \beta(\mathbf{s}, \mathbf{s}'')$, then there exists $H \in \mathcal{H}_3$ such that $\mathbf{s}'' = H\mathbf{s}'$.

This hypothesis is consistent with assumption *A₄* on the minima of the energy. Now, as $\epsilon \rightarrow 0$, the dominant terms at the denominator of (35) correspond to those σ'' such that $\tilde{\beta}(\sigma, \sigma'') = \min_{\sigma \rightarrow \sigma''} \tilde{\beta}(\sigma, \sigma'')$. By assumption *A₅*, there can be only one state that realizes the minimum, so that the leading term only contains one summand. Hence, the low-temperature limit of (35) is

$$\tilde{\Pi}_0(\sigma, \sigma') = \lim_{\epsilon \rightarrow 0} \Pi(\sigma, \sigma') = \begin{cases} 1 & \text{if } \sigma \rightarrow \sigma' \text{ and } \tilde{\beta}(\sigma, \sigma') = \min_{\sigma''} \tilde{\beta}(\sigma, \sigma'') \\ 0 & \text{otherwise} \end{cases} \quad (36)$$

VI. ANALYSIS OF A SPECIAL MODEL

We present below the analysis of a specific model, meant to describe the opening and disgregation of the capsid from the initial closed state and a final state in which all pentamers have detached from the capsid. In this context, x_i is the radial displacement of the capsomers along their axes (cf. Fig. 2). The model is based on the special form of energy function

$$E(\mathbf{x}) = \sum_{i=1}^{12} f(x_i) + \gamma \sum_{i,j=1}^{12} A_{ij} g(d(x_i, x_j)), \quad \gamma \in \mathbb{R}, \quad (37)$$

where f is the expansion energy and g is the attractive interaction energy, that depends on the squared distance $d : \mathbb{R}^2 \rightarrow \mathbb{R}$ between the capsomers, defined by

$$d(x, y) = x^2 + y^2 - 2xy \cos \alpha, \quad (38)$$

where α is the angle between two neighboring icosahedral axes (cf. Figure 2).

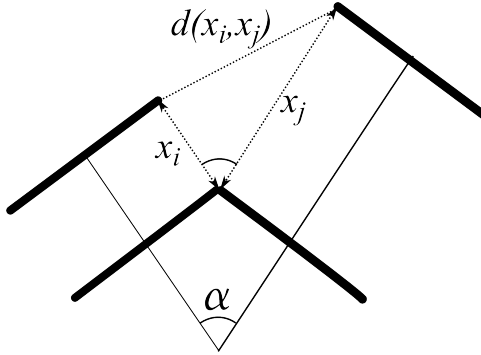


FIG. 2. The squared distance between two capsomers in the problem of the disgregation of the capsid. Schematic side view of two adjacent capsomers translating along their axis by x_i and x_j .

Precisely, we choose the expansion and attractive energies, and the constant γ as

$$f(x) = \begin{cases} (1-x)^2 & x \leq 1 \\ 0 & x > 1 \end{cases}, \quad g(x) = -e^{-ax}, \quad \gamma = 0.1, \quad a = 100. \quad (39)$$

The expansion energy f vanishes for $x \geq 1$, while the attractive energy g has a much shorter radius.

For each given number of detached pentamer, a representative of each icosahedral orbit of admissible states is shown in Fig. 4. Inspection of that figure shows that

- There are multiple states with decreasing number of attached pentagons, but there is only one state (modulo the icosahedral group) with 5 and 4 attached pentamers.

- There are no admissible states with less than 4 attached pentamers. While it is obvious that a single pentamer cannot be attached to anything, even clusters of 4 or more pentamers cannot be stable in real capsids. This is a consequence of working with such a simplified model.
- In each admissible state the pentamer configuration is connected.

In Tables I and II below are listed the half-barriers $\beta(\sigma, \sigma')/2$ between symmetry classes of admissible states for the detachment problem and energy (39). Only the half-barriers between nearest-neighbor states, that correspond to the detachment of a single pentamer, are indicated, with the exception some barriers between states that differ by at least two pentamers. These are written only when they are lower than the barriers between nearest neighbors, or when there is no stable nearest neighbor.

	b	c_1	c_2	c_3	d_1	d_2	d_3	d_4	d_5	e_1	e_2	e_3	e_4	e_5	e_6	e_7	e_8	e_9
a	0.61																	
b		0.42	0.60	0.61														
c_1					0.25	0.42	0.60	0.59										
c_2						0.24	0.42	0.41	0.59									
c_3							0.41											
d_1									0.25	0.41			0.59					
d_2									0.09	0.24	0.41	0.59	0.57					
d_3										0.23	0.40		0.24			0.41		
d_4										0.08		0.40	0.25	0.57	0.41			
d_5											0.23	0.22			0.40			

TABLE I. Half-barriers between states a to e_9 .

Inspection of I and II shows that the lowest barrier between a state and its out neighbors mostly corresponds to the detachment of one of the pentamers with the lowest number of attached neighbors. Computing the non-zero entries of the zero-temperature shows that the most probable transition path from the closed to the open state is

$$a \rightarrow b \rightarrow c_1 \rightarrow d_1 \rightarrow e_1 \rightarrow f_1 \rightarrow g_1 \rightarrow h \rightarrow i, \quad (40)$$

with the same labels as in Figure 4. Figure 3 shows a realization of the most probable transition path.

	f_1	f_2	f_3	f_4	f_5	f_6	f_7	g_1	g_2	g_3	g_4	g_5	h	i	j
e_1	0.24	0.57			0.41										
e_2	0.09		0.56		0.24										
e_3		0.39			0.08										
e_4		0.22	0.07	0.22		0.36									
e_5			0.09			0.37				0.0484					
e_6			0.23	0.39	0.38	0.08									
e_7				0.07		0.20									
e_8					0.22	0.37		0.0475							
e_9		0.21			0.20										
f_1							0.09	0.24	0.23	0.55					
f_2									0.07		0.02				
f_3										0.21	0.05				
f_4										0.07	0.06				
f_5												0.01			
f_6								0.08		0.38					0.002
f_7															
g_1											0.23				
g_2											0.08				
g_3											0.08				
g_4												0.02			
g_5												0.02			
h												0.07			
i													0.05		

TABLE II. Half-barriers between states f_1 to j .

VII. FLUCTUATIONS NEAR EQUILIBRIUM

Linearization of the dynamical system (9) near equilibria gives information on the correlation between the fluctuations of the building blocks of the system.

Consider an admissible state \mathbf{s} and the corresponding equilibrium $\hat{\mathbf{x}}(\mathbf{s})$. The Hessian

$$K = K(\mathbf{s}) = \nabla \nabla E(\hat{\mathbf{x}}(\mathbf{s})),$$

of the energy at this point is positive definite by assumption (cf. (20)), and, using (2), (3) and (26), we see also that

$$R^\top K(\mathbf{s})R = K(\mathbf{s}), \quad \forall R \in \text{Fix}(\mathbf{s}). \quad (41)$$

Fluctuations near the stable equilibrium $\hat{\mathbf{x}}(\mathbf{s})$ are ruled by the linearized system

$$d\mathbf{x} = -K\mathbf{x}dt + \epsilon d\mathbf{W}, \quad K = K(\mathbf{s}). \quad (42)$$

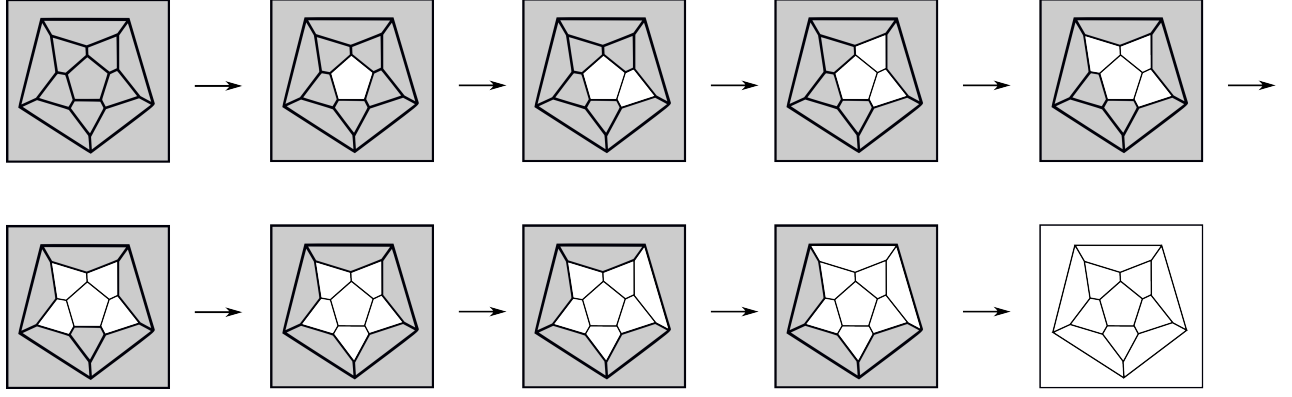


FIG. 3. Minimum energy path for the energy (39). White pentagons are detached.

Assuming the initial condition to be constant or normally distributed, the explicit solution of (42) is a Gaussian process given by (see [29])

$$\mathbf{x}(t) = e^{-tK} \left(\mathbf{x}_0 + \int_0^t e^{zK} d\mathbf{W}(z) \right). \quad (43)$$

The expectation $\mathbf{m} = \mathbf{m}(t) := \mathbb{E}[\mathbf{x}(t)]$ and the covariance matrix $P(t)$ of $\mathbf{x}(t)$, are solutions of the linear ODEs

$$\begin{cases} \dot{\mathbf{m}} = -K\mathbf{m}, \\ \dot{P} = -KP - PK + \epsilon^2 I. \end{cases} \quad (44)$$

The solution of (44)₁ is immediate and it is given by

$$\mathbf{m}(t) = e^{-tK} \mathbf{m}(0). \quad (45)$$

We find the explicit solutions of (44)₂ using some results from matrix algebra. We associate with a matrix $B \in GL(n, \mathbb{R})$ the (column) vector $v(B) \in \mathbb{R}^{n^2}$ of its entries:

$$v(B) := (B_{11}, B_{12}, \dots, B_{1n}, A_{21}, \dots, B_{nn})^T.$$

The following property holds for every $B, C, D \in GL(n, \mathbb{R})$ [30]:

$$v(CBD^T) = (C \otimes D)v(B), \quad (46)$$

where \otimes denotes the Kronecker product of matrices. We transform (44)₂ into a vector equation obtaining

$$\begin{aligned} \frac{dv(P(t))}{dt} &= -v(KP) - v(PK) + \epsilon^2 v(I) \\ &= -(K \otimes I)v(P) - (I \otimes K)v(P) + \epsilon^2 v(I) \\ &= -(K \otimes I + I \otimes K)v(P) + \epsilon^2 v(I), \end{aligned}$$

which is a linear non homogenous first order ODE, whose solutions is given by, setting $\tilde{K} = K \otimes I + I \otimes K$,

$$v(P(t)) = e^{-t\tilde{K}} \left(v(P(0)) + \int_0^t e^{z\tilde{K}} v(I) dz \right). \quad (47)$$

Since $K \otimes I$ and $I \otimes K$ commute, we have, using the properties of the Kronecker product (see [31]),

$$\begin{aligned} \exp(\tilde{K}) &= \exp(K \otimes I + I \otimes K) = \exp(K \otimes I) \exp(I \otimes K) \\ &= (\exp(K) \otimes I)(I \otimes \exp(K)) = \exp(K) \otimes \exp(K). \end{aligned}$$

Using properties (46), equation (47) becomes

$$\begin{aligned} v(P(t)) &= (e^{-tK} \otimes e^{-tK}) \left(v(P(0)) + \epsilon^2 \int_0^t e^{zK} \otimes e^{zK} v(I) dz \right) \\ &= (e^{-tK} \otimes e^{-tK}) \left(v(P(0)) + \epsilon^2 \int_0^t v(e^{zK} I e^{zK}) dz \right) \\ &= (e^{-tK} \otimes e^{-tK}) v \left(P(0) + \epsilon^2 \int_0^t e^{zK} I e^{zK} dz \right) \\ &= v \left\{ e^{-tK} \left(P(0) + \epsilon^2 \int_0^t e^{2zK} dz \right) e^{-tK} \right\}. \end{aligned}$$

Hence, the solution of (44)₂ is given by

$$P(t) = e^{-tK} P(0) e^{-tK} + \epsilon^2 \int_0^t e^{2(z-t)K} dz$$

i.e.,

$$P(t) = e^{-tK} P(0) e^{-tK} + \frac{1}{2} \epsilon^2 K^{-1} (I - e^{-2tK}). \quad (48)$$

The solution $\mathbf{x}(t)$ of (42) has therefore distribution $\mathcal{N}(\mathbf{m}(t), P(t))$. Since K is positive definite, we have

$$\lim_{t \rightarrow +\infty} \mathbf{m}(t) = \mathbf{0}, \quad \lim_{t \rightarrow +\infty} P(t) = \frac{1}{2} \epsilon^2 K^{-1}.$$

Hence, $\mathbf{x}(t)$ converges in distribution to a Gaussian random variable \mathbf{X} with mean $\mathbf{m} = \mathbf{0}$ and covariance matrix $Q = \frac{\epsilon^2}{2} K^{-1}$.

We point out that this result agrees with the LDT framework. In fact, the quasipotential of (42) as in (12) in the basin of attraction of \mathbf{x}_0 is given by $V(\mathbf{x}) = \mathbf{x} \cdot K \mathbf{x}$. It follows from (13) that the stationary distribution $p(\mathbf{x})$ of (42) is asymptotically given by

$$p(\mathbf{x}) \asymp \frac{1}{Z} \exp \left(-\frac{V(\mathbf{x})}{\epsilon^2} \right) = \frac{1}{Z} \exp \left(-\frac{\mathbf{x} \cdot K \mathbf{x}}{\epsilon^2} \right), \quad (49)$$

which is the density of a Gaussian distribution $\mathcal{N}(\mathbf{0}, \frac{1}{2}\epsilon^2 K^{-1})$. Here Z is a normalization constant.

The limiting distribution $p(\mathbf{x})$ has important consequences. Recall that, given three continuous random variables X , Y and Z with joint density distribution $p_{XYZ}(x, y, z)$, we say that X is *conditionally independent of Y given Z* , and write $X \perp Y|Z$, if and only if

$$p_{XY|Z}(x, y|z) = p_{X|Z}(x|z)p_{Y|Z}(y|z).$$

Let $\mathbf{X} = (X_1, \dots, X_n) \sim \mathcal{N}(\mathbf{m}, Q)$ be a multivariate normal distribution. The *concentration matrix* C of \mathbf{X} is the inverse of the covariance matrix Q (provided that $\det(Q) \neq 0$). The entries of C measure the correlation between the components. In particular, the *partial correlation coefficients* are given by

$$\rho_{ij|\mathcal{S}\setminus\{i,j\}} := -\frac{(Q^{-1})_{ij}}{\sqrt{(Q^{-1})_{ii}(Q^{-1})_{jj}}}. \quad (50)$$

where $\mathcal{S} = \{1, \dots, n\}$. Moreover, the following hold:

$$X_i \perp X_j | \mathbf{X}_{\mathcal{S}\setminus\{i,j\}} \iff (Q)_{ij}^{-1} = 0. \quad (51)$$

If condition (51) is satisfied, then \mathbf{X} is known as a *Gaussian Markov random field* [32]. In our case, the concentration matrix of \mathbf{x} is $\frac{2}{\epsilon^2}K$, and we have, from (50)

$$\rho_{ij|\mathcal{S}\setminus\{i,j\}} = -\frac{K_{ij}}{\sqrt{K_{ii}K_{jj}}}. \quad (52)$$

Now, from the expression (6), it follows that

$$\text{if } s_i = \hat{x}_i = 1 \text{ then } K_{ij}(\mathbf{s}) = 0, \quad \text{for } j \neq i, \quad (53)$$

since, by A_2 , $g(x, y)$ and all its derivatives vanish whenever one of its arguments is 1. Moreover, if $\hat{x}_i < 1$, so that $s_i = 0$, then

$$K_{ii}(\mathbf{s}) = f''(\hat{x}_i) + 2\gamma \sum_{j:s_j=0} A_{ij}g_{11}(\hat{x}_i, \hat{x}_j). \quad (54)$$

A first consequence of (6), (52) and (53) is that, at an admissible state, two pentamers are correlated if and only if they are adjacent in the configuration \mathbf{s} . In other words, the random variable \mathbf{x} is a Gaussian graphical model with graph the subgraph of the icosahedral graph induced by the vertices with zero components of \mathbf{s} .

In turn, (54) shows that the diagonal elements K_{ii} of the Hessian depend only on the pentamers adjacent to i in the state \mathbf{s} . Actually, (54) suggests that K_{ii} is larger the greater is the connectivity of pentamer i in the state \mathbf{s} . Hence, a pentamer with high connectivity has a small correlation coefficient with its neighbors.

VIII. CONCLUSIONS

Large deviations theory for stochastic differential equations is based on the notion that arbitrarily small stochastic perturbations are able to lead any system out of equilibrium, over sufficiently long times, and minimum energy paths allow to determine the most probable transition paths between metastable states: the resulting Markov chain on the set of minima completely describes the stochastic dynamics on the energy landscape. In this work we have used this approach to get insights into the process by which viral capsids change configuration, in either maturation or infection.

Our analysis supports the conjecture that destabilization occurs by a cascade of local events: in fact, the energy is the sum of a destabilizing term on each pentamers, which does not depend on its neighbors, and a cohesive term opposing the transition, which accounts for the interactions between adjacent pentamer. Destabilization is the result of the competition between these terms: the expansive energy decreases whenever a pentamer changes state, but this requires to provide an amount of cohesive energy proportional to the number of bonds broken in the process. This suggests that the cascade occurs by destabilization of those pentamer that have less bonds, and therefore have to pay less energy to detach. Simulations confirm the intuitive picture above: for instance, in the parameter range in which we are working, whenever a pentamer has only one bond left, it switches to its final configuration, because the energy gained by this process is larger than the amount lost by bond breaking.

For simplicity, we have computed in this paper just the zero-temperature transitions, i.e., the limit of the transition matrix of the Markov chain as $\epsilon \rightarrow 0$, but the procedure is fully general and allows to study all transitions between metastable states.

In order to further explore how random fluctuations affect the stability of a complex interacting structure, we have also focused on the linearized system. Clearly, the destabilization dynamics of strongly nonlinear, but the analysis of its linearization in the neighborhood of an attractor yields interesting information. First of all, the process is Gaussian

and its limit distribution is a multivariate normal. The concentration matrix C is proportional to the Hessian of the energy at equilibrium, which has nonzero entries only when two pentamers are adjacent. This is a first confirmation of the effect of locality on this model, but the point is that this allows to compute the conditional correlation coefficients between fluctuations at adjacent pentamers. This shows that if a pentamer i has many unbroken bonds and H_{ii} and C_{ii} are large, the fluctuations are highly concentrated at that pentamer, and the correlation between this and adjacent pentamers is small.

On the other hand, when a pentamer i has a small connectivity, the concentration coefficient C_{ii} is small, and the pentamer has large negative correlation coefficients with its neighbors. This means that fluctuations tend to amplify, which is a clue of the destabilization effect.

The procedure described in this paper can be automatized and generalized to any system made of pairwise interacting building blocks, once the interactions are encoded in a simple graph.

ACKNOWLEDGMENTS

We thank R. Kohn for suggesting the use of LDT to study transitions, and E. Vandenberg-Eijnden for valuable comments and suggestions. GI acknowledges support by the Italian GNFM (Progetto Giovani 2016) and GI and PC acknowledge support by the University of Torino (research project 'Modelli Aleatori')).

- [1] F.H.C. Crick, J.D. Watson, Structure of small viruses, *Nature* **177**, 473-475 (1956).
- [2] R. Zandi, D. Reguera, Mechanical properties of viral capsids, *Physical Review E* **72**, 021917 (2005).
- [3] T.J. Tuthill, K. Harlos, T.S. Walter, K.J. Knowles, E. Groppelli, D.J. Rowlands, D.I. Stuart, E.E. Fry, Equine rhinitis A virus and its low pH empty particle: clues towards an aphthovirus entry mechanism?, *PLoS Pathogens* **5**/10, e1000620 (2009).
- [4] S.E. Bakker, E. Groppelli, A.R. Pearson, P.G. Stockley, D.J. Rowlands, N.A. Ranson, Limits of structural plasticity in a picornavirus capsid revealed by a massively expanded Equine Rhinitis A Virus particle, *Journal of Virology* **88**/ 11, 6093-6099 (2014).

[5] N. Verdaguer, D. Blaas, I. Fita. Structure of Human Rhinovirus Serotype 2 (HRV2), *Journal of Molecular Biology* **300**, 1179-1194 (2000).

[6] E. A. Hewat, E. Neumann, D. Blaas, The concerted conformational changes during Human Rhinovirus 2 uncoating, *Molecular Cell* **10**, 317326 (2002).

[7] D. Garriga, A. Pickl-Herk, D. Luque, J. Wruss, J. R. Casto, D. Blaas, N. Verdaguer, Insights into minor group Rhinovirus uncoating: the X-ray structure of the HRV2 empty capsid, *PLoS Pathogens* **8**/1, e1002473 (2012).

[8] Y. Cao, A single-molecule view on the disassembly of Tobacco Mosaic Virus, *Biophysics Journal* **105**/12, 2615-2616 (2013).

[9] I. Gertsman, E.A. Komives, J.E. Johnson, HK97 maturation studied by crystallography and H/ 2 H exchange reveals the structural basis for exothermic particle transitions, *Journal of Molecular Biology* **397**/2, 560-574 (2010).

[10] J.F. Conway, W.R. Wikoff, N. Cheng, R.L. Duda, R.W. Hendrix, J.E. Johnson, A.C. Steven, Virus maturation involving large subunit rotations and local refolding, *Science* **292**, 744-748, (2001).

[11] J.A. Speir, S. Munshi, G. Wang, T. S. Baker, J. E. Johnson, Structures of the native and swollen forms of cowpea chlorotic mottle virus determined by X-ray crystallography and cryo-electron microscopy, *Structure* **3**/1, 6378 (1995)

[12] M. Castellanos, R. Perez, P.J.P. Carrillo, P. J. de Pablo, M. G. Mateu, Mechanical disassembly of single virus particles reveals kinetic intermediates predicted by theory, *Biophysics Journal* **102**/11, 2615-2624 (2012).

[13] W. H. Roos, I. Gertsman, E.R. May, C. L. Brooks III, J. E. Johnson, G.J.L. Wuite, Mechanics of bacteriophage maturation, *Proceedings of the National Academy of Sciences* **109**/7, 2342-2347 (2012).

[14] M.K. Kim, R.L. Jernigan, G.S. Chirikjian, An elastic network model of HK97 capsid maturation, *Journal of Structural Biology* **143**, 107-117 (2003).

[15] P. Cermelli, G. Indelicato, R. Twarock, Nonicosahedral pathways for capsid expansion, *Physical Review E* **88**, 032710 (2013).

[16] G. Indelicato, P. Cermelli, D.G. Salthouse, S. Racca, G. Zanzotto, R. Twarock, A crystallographic approach to structural transitions in icosahedral viruses, *Journal of Mathematical Biology* **64**, 745-773 (2012).

- [17] L.E. Perotti, J. Rudnick, R.F. Bruinsma, and W.S. Klug, Statistical Physics of Viral Capsids with Broken Symmetry, *Physical Review Letters* **115**, 058101 (2015).
- [18] M.I. Freidlin, A. D. Wentzell, *Random Perturbations of Dynamical Systems*, Springer, Dordrecht (2012).
- [19] W. E, W. Ren, E. Vanden-Eijnden, String method for the study of rare events, *Physical Review B* **66**, 052301 (2002).
- [20] W. E, W. Ren, E. Vanden-Eijnden, Minimum action method for the study of rare events, *Communications in Pure and Applied Mathematics* **57** / 5, 637 - 656 (2004).
- [21] T. Grafke, T. Schäfer, E. Vanden-Eijnden, Long-lasting effects of small random perturbations on dynamical systems: theoretical and computational tools, arXiv:1604.03818 (2016).
- [22] R. Kohn, Energy-driven pattern formation, *Proceeding of the International Congress of Mathematicians, Madrid, Spain, 2006, European Mathematical Society*, pp 1-25 (2006).
- [23] C. Godsil, G. Royle, *Algebraic graph theory*, Springer-Verlag, New York (2001).
- [24] H.F. Jones, *Groups, Representations and Physics*, Institute of Physics Publishing (1990).
- [25] E. Zappa, G. Indelicato, A. Albano, P. Cermelli, A Ginzburg-Landau model for the expansion of a dodecahedral viral capsid, *International Journal of Non Linear Mechanics* **56**, 71-78 (2013).
- [26] D. M. Cvetkovic, M. Doob, H. Sachs, *Spectra of graphs: theory and application*, Academic Press, New York (1980).
- [27] M.K. Cameron, Computing Freidlin's Cycles for the Overdamped Langevin Dynamics. Application to the Lennard-Jones-38 Cluster. *Journal of Statistical Physics* **152**/3, 493518 (2013).
- [28] G. Grimmett, D. Stirzaker, *Probability and Random Processes*, Oxford University Press (2001).
- [29] L. Arnold, *Stochastic differential equations: theory and applications*, Wiley-Interscience, New York (1974).
- [30] S. Barnett, Matrix differential equations and Kronecker products, *SIAM Journal on Applied Mathematics* **24**/1, 1-5 (1973).
- [31] R.A. Horn, C.R. Johnson, *Matrix Analysis*, Cambridge University Press (1985).
- [32] S.L. Lauritzen, *Graphical models*, Clarendon Press, Oxford (1996).

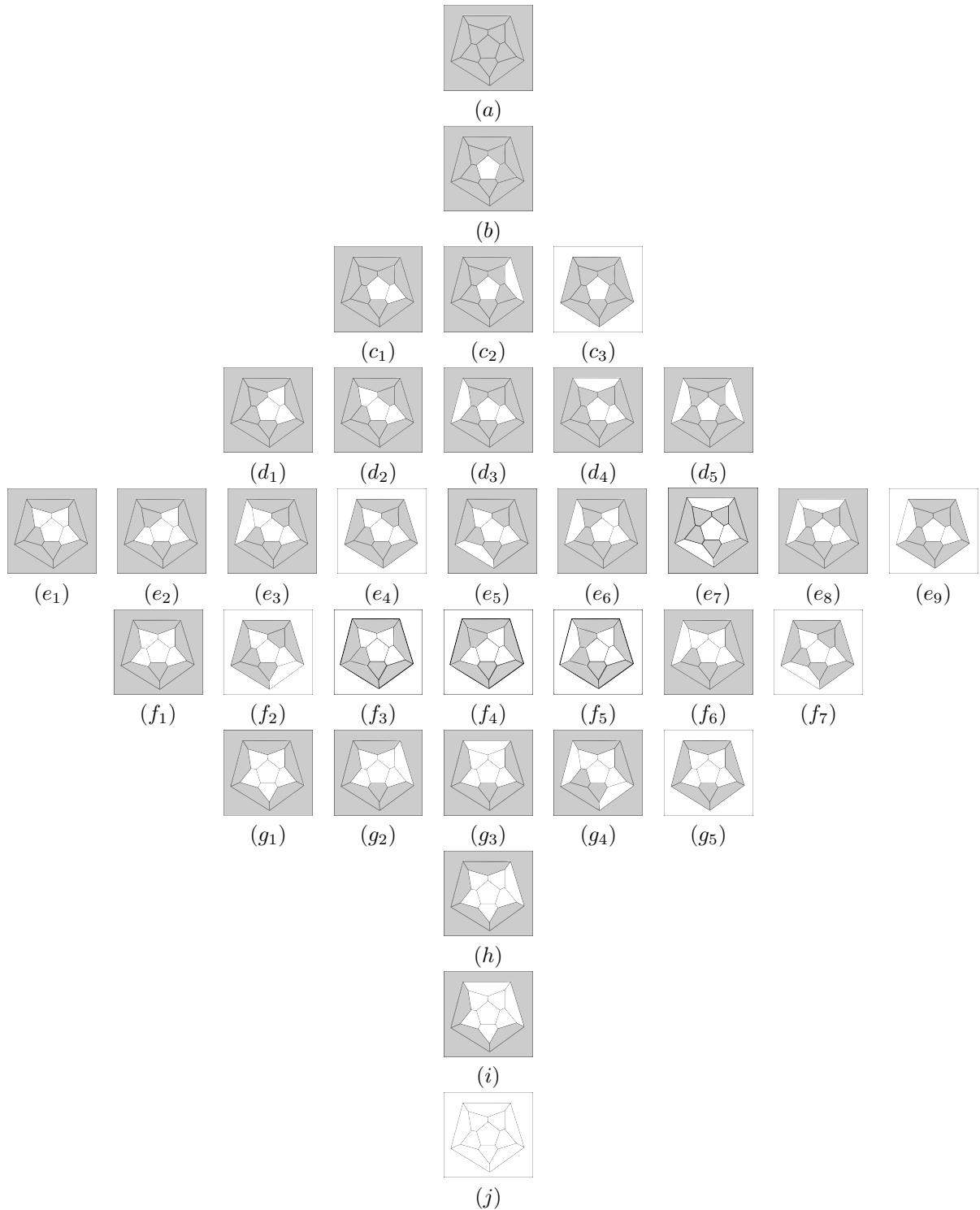


FIG. 4. Representatives of the symmetry classes of admissible states for the energy (39). White pentagons represent detached pentamers. (a) is the closed capsid, (j) is the totally disregulated capsid.